Load Alleviation Potential with Trailing Edge Flaps for Turbines in Wake Operation

Andreas Fischer[1], Helge Aagaard Madsen[1]

[1]Technical University of Denmark, Institute for Wind Energy, asfi@dtu.dk

ABSTRACT

We performed computations with the aeroelastic wind turbine code HAWC2 for the 2.3 NM80 wind turbine in free inflow conditions and in a full wake situation. The added turbulence in the wake flow is modelled with a dynamic wake meandering model. The computations were validated against measurements made during the DAN-AERO MW project. In this project a NM80 wind turbine situated in a small wind farm consisting of 8 turbines was equipped with inflow sensors and pressure tabs along the blade at 4 different radial sections. The inflow velocity and angle towards the blade as well as the normal force were in good agreement in measurement and computation. We applied an ideal flap control algorithm and investigated the fatigue load reduction potential for the blade normal force. The relative fatigue load reduction was the same in free flow condition and in wake operation, but the absolute value of the fatigue loads was higher in wake operation.

1 Introduction

Wind turbines placed in wind farms often operate in the wake of adjacent wind turbines. The wake flow creates turbulence which interacts with the atmospheric turbulence. Hence, the overall inflow turbulence level is increased. It is anticipated that such an operational condition leads also to an increase of the cyclic loads on the blade which cause fatigue damage. It is very much desired to decrease those loads.

In the DAN-AERO MW project [1] a 2.3MW NM80 wind turbine situated in a small wind farm consisting of 8 turbines was heavily equipped with sensors to measure inflow characteristics and blade loads. During the campaign the turbine operated in free inflow conditions as well as in wake situations. We evaluated the spectral characteristics of the inflow velocity and the blade normal force. The data set shows how those characteristics are changed by the wake. It is also used to validate the Dynamic Wake Meandering (DWM) [2], [3] model which was recently implemented in the aero-elastic code HAWC2 [4] and validated against full scale measurements [5]. This model describes in a simple and computationally effective way how the wake of a wind turbine increases the turbulence level of the atmospheric flow.

It was demonstrated that trailing edge flaps in combination with inflow measurements on the blade are an effective measure to alleviate fatigue loads [6]. An ideal feed forward control algorithm using the measured relative velocity and angle of attack at a blade section to control the normal force was developed. In this paper the fatigue load reduction potential of trailing edge flaps for wind turbines operating in wake situations is demonstrated.

2 Methods

2.1 DAN AERO measurements

The measurements presented in this paper were carried out in the DAN-AERO MW project, funded by the Danish Energy Research programme EFP-2007 under contract Journal no. 33033-0074. The project was carried out in the period from March 2007 to December 2009 in corporation between Risø DTU, now DTU Wind Energy, and the companies LM Wind Power, Vestas Wind Systems, Siemens Wind Power and DONG Energy. More details of the experiment are presented in [1].
One blade of a NEG-Micon NM80 turbine was heavily equipped with measurement sensors. The three bladed turbine has a rotor diameter of 80m and the hub height is 57m, the rated power is 2.3MW. The blade contained among other sensors pressure tabs at radial position r=13m, 19m, 30m and 37m and four five-hole pitot tubes at radial position r=14.5m, 20.3m, 31m and 36m, figure 1.

Figure 1: The blade of the NM80 turbine equipped with measurement devices.

The turbine was placed in a small wind farm of 8 turbines at Tjæreborg Enge, about 1km away from the west coast of Jutland, Denmark, figure 2. The other turbines in the wind farm are of the same type. The nearest turbine was at a distance of 253m away from the NM80, the one furthest away at a distance of 884m. Calculations were made in [7] to predict for which wind directions the NM80 operates in the wake of another turbine and how much of the swept area of the rotor is influenced. The calculations were based on geometrical considerations and wake diameter variations depending on the induction. Our choice of free inflow and full wake cases

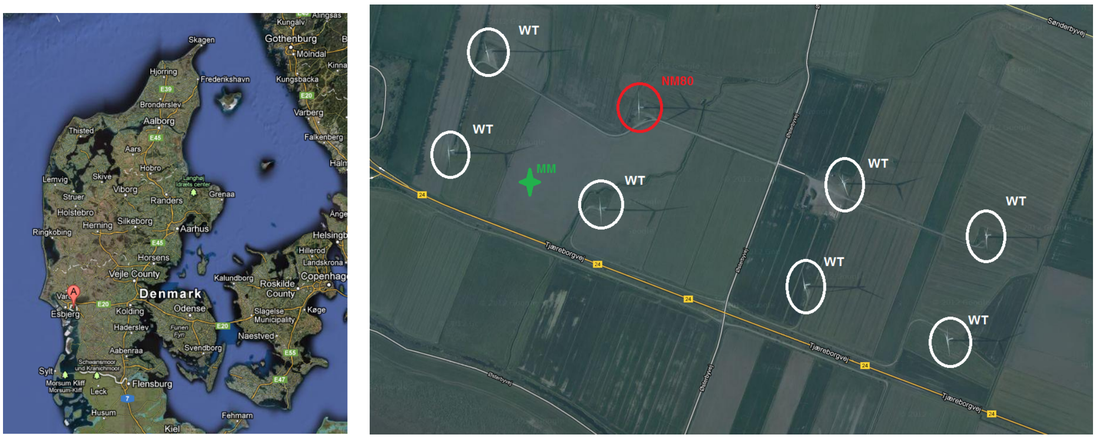

(a) Location in Denmark (b) Wind Farm

Figure 2: Map of the wind farm in Tjæreborg Enge. NM80: NM80 turbine, WT: wind turbine, MM: meteorological mast.

was based on those calculations.
A meteorological mast was situated about half way between the two turbines southwest of the NM80. The mast was equipped with cup anemometers and wind vanes at a height of 17m, 28.5m, 41m, 57m, 77m and 93m to provide wind speed and direction measurements. Additionally there were 3 sonic anemometers at altitude 17m, 57m and 93m. They provided measurements of the three components of the wind vector. Those sensors are suitable to provide the turbulence intensity of the inflow.

2.2 Aero-elastic model

The simulations in this work were performed with the aero-elastic code for horizontal axis wind turbines HAWC2 [4]. The code was developed at DTU wind energy over more than 10 years. The structural part of the code is based on a multibody formulation. Arbitrary large rotation of the bodies can be handled. The bodies are assembled of Timoshenko beam elements. The aerodynamic model is based on the classic blade element momentum theory. But the theory was extended to include the effects of dynamic, skewed and sheared inflow as well as large deflections and dynamic stall of the blades. The code can simulate trailing edge flaps on the blade.
The dynamic wake meandering model (DWM) is an essential part of this work. The theoretical background of this model is described in [2], the implementation in the HAWC2 code and tuning of the model parameters in [3]. The DWM adds the turbulence generated by the wake of another turbine linearly to the ambient inflow turbulence. The wake generated turbulence consists of two parts, the meandering of the velocity deficit driven by the large turbulence scales in the atmospheric flow and the small scale wake added turbulence generated by the sheared velocity profile in the wake and the shed blade bound vorticity.
The flow conditions as experienced during the measurements were described as closely as possible in the simulations, i.e. the wind velocity profile and the inflow turbulence intensity were

adjusted to match the measured ten minutes average. Inflow turbulence is described by the Mann turbulence model [8]. The structural model for HAWC2 of the NM80 turbine is described in [9]. The operational conditions of the NM80 turbine, i.e. the rotational speed of the rotor and the pitch angle setting, were monitored as well in the experiment and matched in the computations. Note that the turbine operated with constant rotational speed.

2.3 Fatigue Load Calculation

The equivalent fatigue load range number S_{eq} and the corresponding number of load range occurrences n_{eq} are defined according to the classical theory of Palmgren-Miner and Wöhler. It was derived in [10] and is given by

$$S_{eq} = \left(\frac{\sum n_i S_i^m}{n_{eq}} \right)^{1/m}. \tag{1}$$

The set of fatigue load ranges S_i and their number of occurrence n_i for a given load time trace are calculated with the Rainflow counting algorithm [11]. The Wöhler exponent m is a parameter describing the characteristic of the specific material. For wind turbine blades a value of $m = 10$ is normally used.
The equivalent fatigue load range number S_{eq} gives the range of a periodic load which causes the same fatigue damage as the set of fatigue load ranges S_i, n_i when occurring n_{eq} times. If we have a load time trace of of 600s duration and set $n_{eq} = 600$, the equivalent fatigue load range number can be interpreted as a sinusoidal load fluctuation with a frequency of 1Hz and we denote it with S_1.

3 Results

3.1 Inflow Conditions

The data base of the measurements in the DAN AERO project [1] contained two 10 minute measurement series with very similar inflow condition in terms of wind speed, shear and turbulence intensity, but the wind coming from very different direction, table 1. The flow conditions of

	wake situation 21/07/2009 13:10	free inflow situation 19/08/2009 12:30
wind speed at hub [m/s]	7.05	7.21
turbulence intensity at hub [%]	9	7
shear exponent [-]	0.09	0.15
wind direction at hub [deg]	256	161

Table 1: Wind conditions measured by the met mast.

the July measurement resulted in a situation where the NM80 turbine operates in the wake of turbine 1. The wake shadow coverage was estimated with the method described above, figure 3. According to the computation, 96% of the rotor area is in the wake shadow of the upstream

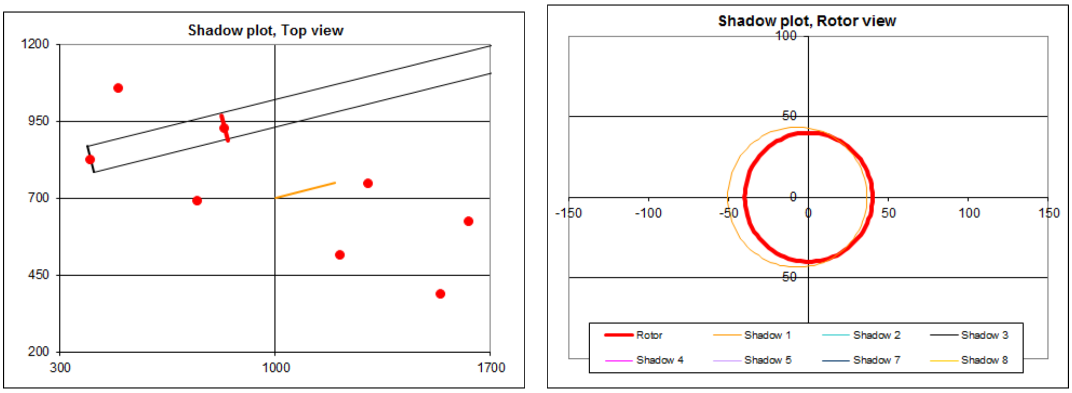

(a) Top view.

(b) Rotor view.

Figure 3: Wake shadow for measurement on July 21st, 2009, 13:10.

turbine. Turbine 1 is at a distance of 448m away from the NM80 turbine. This corresponds to 5.6 times the rotor diameter.

In the august measurement the flow comes from a direction so that the turbine operates in free flow conditions, figure 4. The corridor for free flow conditions is very wide for this specific

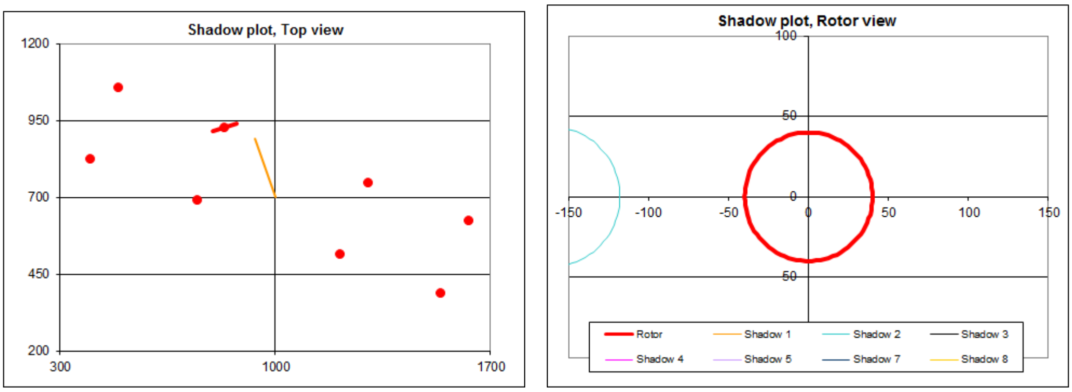

(a) Top view.

(b) Rotor view.

Figure 4: Wake shadow for measurement on August 19th, 2009, 12:30.

range of wind directions. Even though there is an uncertainty in the wake prediction method, in this situation wake interaction is very unlikely.

3.2 Spectral Analysis of Inflow and Blade Normal Force

The spectral characteristics of the inflow to the blade is changed if the turbine operates in wake. We compare the measured and computed inflow characteristics for two blade sections, approximately r=20m and r=31m, in figure 5 and 6. Note that the exact measurement position and the computational node do not exactly coincide. All the spectra are characterized by peaks at

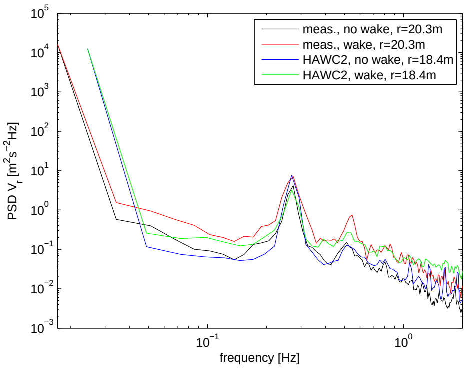

(a) radial position r=20m

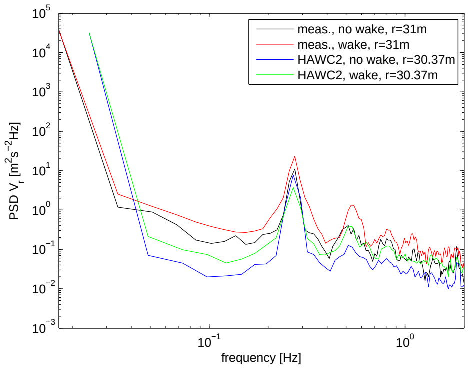

(b) radial position r=31m

Figure 5: PSD of the relative velocity.

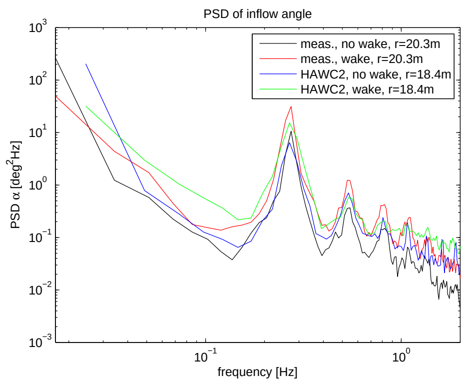

(a) radial position r=20m

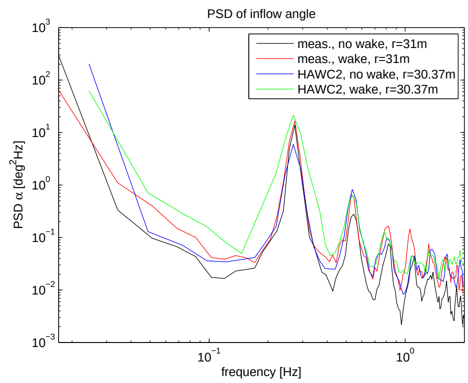

(b) radial position r=31m

Figure 6: PSD of the inflow angle.

multiples of the rotational frequency of the rotor. At the inner rotor position we observe higher spectral levels of the inflow velocity and inflow angle when the turbine operates in wake situation. For free inflow conditions the agreement between measured and computed inflow velocity spectrum is excellent. In full wake situation minor differences occur. The characteristic peak at 1 times the rotational frequency is broader in the measurement. For high frequencies the computation gives higher levels than the measurement. For the inflow angle the difference between measurement and computation are more significant. The size of the peak at a frequency equal to the rotational frequency is well predicted by the computation in both cases. But in the case of free inflow the spectral level of the computations is higher than the one of the measurements for higher frequencies. In wake situation the level for higher frequencies is overestimated, but the amplitude of the characteristic peaks is underestimated.

At the outer rotor position, the measured inflow velocity shows much higher turbulence levels as the computed one in both cases. In full wake situation the spectral peak corresponding to the

rotational frequency is broader in the measurement than in the computation. For the inflow angle the situation is reversed. The results of the computation have higher spectral levels. In full wake situation the width of the peak at the rotational frequency is broader in the computation than in the measurement.
The normal sectional blade force is displayed in figure 7. The agreement between measurement

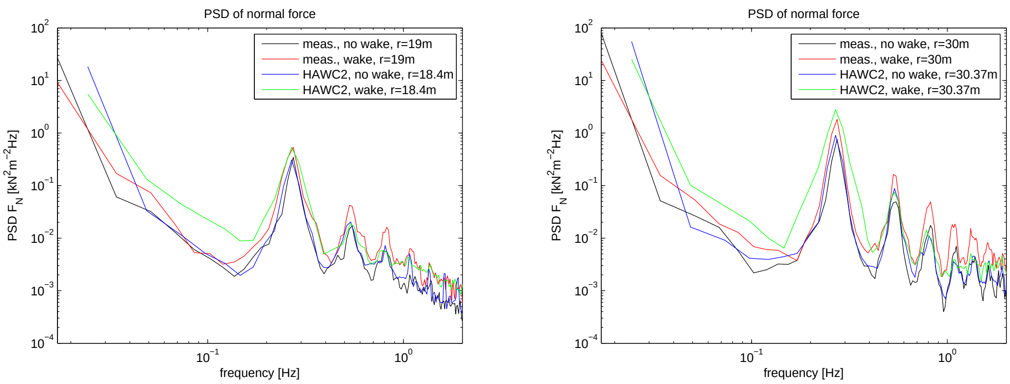

(a) radial position r=19m (b) radial position r=30m

Figure 7: PSD of the blade normal force.

and computation at both radial positions is excellent in free flow conditions. In full wake situation the level of the spectrum is higher than the level in free flow conditions. The computations give higher values than the measurements in the low frequency range and the peak at the rotational frequency is broader. The low frequency range is mainly influenced by the large scale movement of the turbine wake. The meandering turbulence level is normally the same as the one of the atmospheric turbulence. It can be reduced to give a better agreement with the measurement of the normal force. In the computations presented here the meandering turbulence level was slightly decreased to 7% instead of 9% (measured value of the atmospheric turbulence).
For higher frequencies the amplitude of the peaks corresponding to multiples of the rotational frequency are underestimated in level by the computation compared to the measurement. This regime is characterized by the small scale turbulence generated in the wake. The wake generated small scale turbulence might be underestimated be the DWM model.

3.3 Fatigue Load Analysis

Figure 8(a) shows the 1Hz equivalent fatigue load of the normal force at different blade positions. The fatigue loads were computed with a Wöhler exponent of $m = 10$. They are highly non-linear and due to some variation when computed for 10 minutes time series. In the regard of that the measurement and computation is in good agreement for the free inflow case. The computation overpredicts only slightly. The fatigue loads increase significantly if the turbine operates in the wake. The computation overpredicts also in this case, but the relative increase of the fatigue loads is well predicted, figure 8(b). This is due to the increased level of the blade normal force in the low frequency range in the computations. Low frequency fluctuations with high amplitude

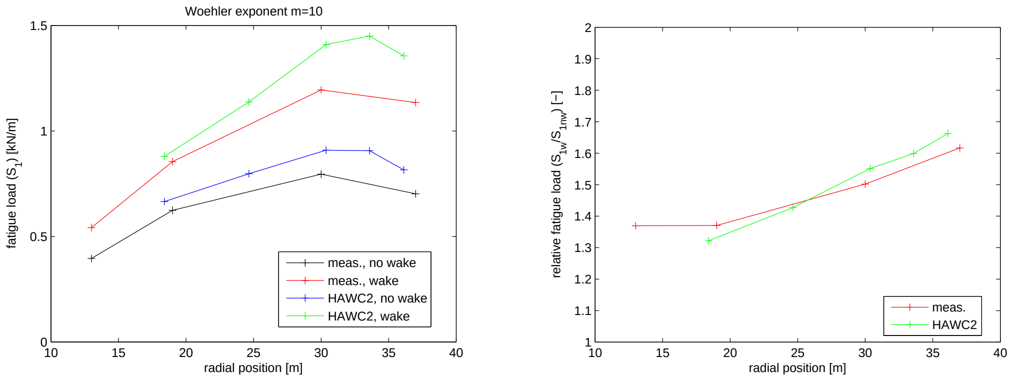

(a) absolute (b) normalized with free flow condition value

Figure 8: 1Hz equivalent fatigue loads of the normal force of the NM80 wind turbine.

count strongly to the equivalent fatigue load when a high Wöhler exponent is applied.
The spectrum of the fatigue load cycles at radial position r=19m and r=30m is shown in figure 9. The size of the second peak in the spectrum at high load ranges dictates mainly the value of the

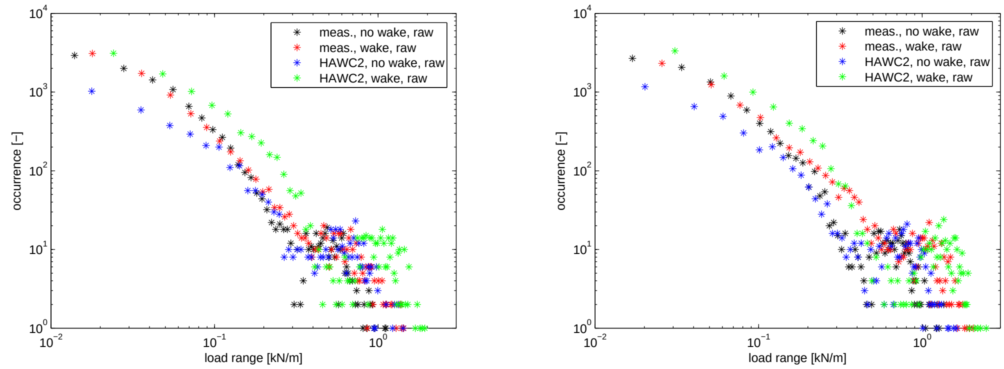

(a) r=19m (b) r=30m

Figure 9: Fatigue load cycle spectrum.

equivalent fatigue load because of the high Wöhler exponent. The behaviour of the spectrum in the low load range is of little importance. The computations show higher load ranges than the measurements.
To illustrate the load reduction potential of flaps we applied the control algorithm [6] to the time series of the blade normal forces by using the measured inflow velocity and angle at radial position 20.3m in the case of measurement data and at 18.4m in case of computations. This was the closest node in the BEM model to the measurement position. The equivalent fatigue load of the controlled normal force S_{1c} was computed and the absolute fatigue load reduction was quantified with $1-S_{1c}/S_1$, figure 10(a). We applied an ideal filter to the blade normal force and computed the equivalent fatigue load S_{1f} for the filtered time series. The maximum obtainable

fatigue load reduction can then be quantified as $1 - S_{1f}/S_1$, the dashed lines in figure 10(a). The fatigue load reduction relative to the absolute maximum $(S_1 - S_{1c})/(S_1 - S_{1f})$ are shown in figure 10(b).

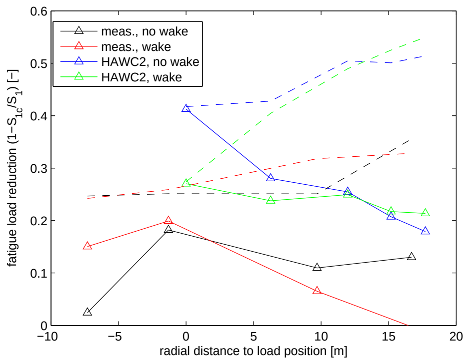

(a) absolute, dashed line: Maximum obtainable fatigue load reduction

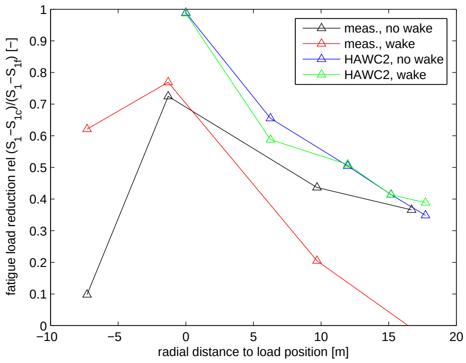

(b) relative to maximum obtainable fatigue load reduction

Figure 10: Fatigue load reduction with ideal flap control.

The achieved fatigue load reduction is different for free inflow condition and full wake operation in the computations. But relative to the absolute maximum of the fatigue load reduction the achieved reductions are similar in both cases. The variation of the absolute values is due to the concrete time history of the inflow turbulence and is not influenced by wake operation. The fatigue loads were evaluated based on 10 min time series. It would be better to evaluate fatigue loads based on 1 hour time series. This was not possible in the case of the measurement and avoided in the computation in order to be consistent.

For the measured normal force a much lower fatigue load reduction was achieved compared to the computations. This could be due to added noise to the time series by the measurement system. However, the measurements show that a considerable fatigue load reduction is possible and the amount of reduction is the same in free flow conditions as in full wake operation.

4 Discussion

In the DAN AERO experiment a huge data set of full scale wind turbine aerodynamic and blade loading data was collected. The data set contained two measurements with similar wind conditions, but the NM80 wind turbine once operating in free inflow and once in a full wake situation. We investigated the spectral characteristics of the blade inflow velocity and angle as well as the blade normal force to evaluate the fatigue loads. The measured data was compared with computations with the HAWC2 aero-elastic code. The code includes a model describing the dynamic meandering of the wake (DWM).

The spectral level of the inflow velocity was in general slightly underpredicted by the HAWC2 code in both cases, except for high frequencies at the inboard part of the rotor. Here the level is higher than the one of the measurements. The spectral level of the inflow angle was in general slightly overestimated, but in wake operation, the amplitude of the spectral peaks at multiples of the rotational frequency are underestimated.

For free flow condition the normal force spectra of computation and measurement were in excellent agreement. In wake operation, the normal force was overestimated in the low frequency range. Hence, we adjusted the turbulence level of the large scale movement of the wake. In the high frequency range the normal force level was underestimated by the computation. This domain is governed by the small turbulence scales in the wake.

The fatigue loads are much higher in wake operation compared to free inflow situation. This was confirmed both by measurement and computation, even though the computation overestimated the fatigue loads compared to the measurement. However, the relative increase of the fatigue loads due to wake operation was predicted correctly.

The fatigue load reduction potential by flaps is approximately the same in wake and free inflow situation. Due to the higher absolute value of the fatigue loads is the reduction more valuable in the case of wake operation. The fatigue load reduction potential predicted by the computations could not be obtained for the measured time series. Further investigation is necessary here.

References

[1] Madsen HA, Bak C, Paulsen US, Gaunaa M, Fuglsang P, Romblad J, Olesen NA, Enevoldsen P, Laursen J, Jensen L. The DAN-AERO MW Experiments: Final report. *Tech. Rep. Risø-R-1726(EN)*, Risø-DTU, Roskilde, Denmark September 2010.

[2] Larsen GC, Madsen HA, Thomsen K, Larsen TJ. Wake meandering - a pragmatic approach. *J. of Wind Energy* 2008; **11**:377–395.

[3] Madsen HA, Larsen GC, Larsen TJ, Troldborg N. Calibration and Validation of the Dynamic Wake Meandering Model for Implementation in an Aeroelastic Code. *J. Sol. Energy Eng.* 2010; **132**(4).

[4] Larsen TJ, Hansen AM. How to HAWC2, the users manual. *Tech. Rep. Risø-R-1597(ver.4-3)(EN)*, DTU Wind Energy, Roskilde, Denmark April 2012.

[5] Larsen TJ, Madsen HA, Larsen GC, Hansen KS. Validation of the dynamic wake meander model for loads and power production in the Egmond aan Zee wind farm. *J. Wind Energy* 2012; .

[6] Fischer A, Madsen HA. Investigation of the maximum load alleviation potential using trailing edge flaps controlled by inflow data. *The science of making torque from wind Conf. (EWEA)*, Oldenburg, GE, 2012.

[7] Bak C, Madsen HA, Hansen P, Rasmussen M, Fuglsang P, Romblad J, Olesen NA. DANAERO MW: Measurement campaigns on the NM80 2.3MW wind turbine at Tjæreborg 2009. *Tech. Rep. Risø-I-3046(EN)*, Risø-DTU, Roskilde, Denmark November 2010.

[8] Mann J. The spatial structure of neutral atmospheric surface-layer turbulence. *J. of Fluid Mech.* 1994; **273**:141–168.

[9] Hansen MH, Fuglsang P, Thomsen K. Aeroelastic modeling of the NM80 turbine with HAWC. *Tech. Rep. Risø-I-2017(EN)(Confidential)*, Risø-DTU, Roskilde, Denmark December 2004.

[10] Thomsen K. The Statistical Variation of Wind Turbine Fatigue Loads. *Tech. Rep. Risø-R-1063(EN)*, Risø National Laboratory, Roskilde, Denmark September 1998.

[11] Matsuishi M, Endo T. Fatigue of metals subjected to varying stress. Paper presented to Japan Soc Mech Engrs, Jukvoka, Japan 1968.